 doi:10.20944/preprints201809.0486.v1

Overexpression of AhHDA1 results in retarded growth of hairy roots and altered cell metabolism in *Arachis hypogaea*

Liangchen Su[1,2#], Shuai Liu[1#], Xing Liu[1], Baihong Zhang[1], Meijuan Li[1], Lidan Zeng[1], Ling Li[1,*]

Author affiliations:

[1]Guangdong Provincial Key Laboratory of Biotechnology for Plant Development, School of Life Sciences, South China Normal University Guangzhou, China

[2]Department of Bioengineering, Zhuhai Campus of Zunyi Medical University, Zunyi, Guizhou, China

Author email addresses:

Liangchen Su: sksky163@163.com, Shuai Liu: 408152101@qq.com, Xing Liu: 10150926@qq.com, Baihong Zhang: 1311369961@qq.com, Meijuan Li: 929722415@qq.com, Lidan Zeng: 2036428216@qq.com

[#]These authors have contributed equally to this work.

*Correspondence:

Ling Li, Guangdong Provincial Key Laboratory of Biotechnology for Plant Development, School of Life Sciences, South China Normal University, No. 55, Zhongshan Avenue West, Tianhe District, Guangzhou 510631, China; liling502@126.com

Preprints (www.preprints.org) | NOT PEER-REVIEWED | Posted: 25 September 2018 doi:10.20944/preprints201809.0486.v1

Abstract

Peanut (*Arachis hypogaea*) is a crop plant with high economic value, but the epigenetic regulation of its growth and development has only rarely been studied. The peanut histone deacetylase 1 gene (*AhHDA1*) has been isolated and is known to be ABA- and drought-responsive. In this paper, we investigate the role of *AhHDA1* in more detail, focussing on the effect of altered *AhHDA1* expression in hairy roots at both the phenotypic and transcriptional levels. *Agrobacterium rhizogenes*-mediated transformation of *A. hypogaea* hairy roots was used to analyse how overexpression or RNA interference of *AhHDA1* affects this tissue. In both types of transgenic hairy root, RNA sequencing was adopted to identify genes that were differentially expressed, and these genes were assigned to specific metabolic pathways. *AhHDA1*-overexpressing hairy roots were growth-retarded after 20 d in vitro cultivation, and superoxide anions and hydrogen peroxide accumulated to a greater extent than in control or RNAi groups. Overexpression of *AhHDA1* is likely to accelerate flux through various secondary synthetic metabolic pathways in hairy roots, as well as reduce photosynthesis and oxidative phosphorylation. Genes encoding the critical enzymes caffeoyl-CoA O-methyltransferase (*Araip.XGB85*) and caffeic acid 3-O-methyltransferase (*Araip.Z3XZX*) in the phenylpropanoid biosynthesis pathway, chalcone synthase (*Araip.B8TJ0*) and polyketide reductase (*Araip.MKZ27*) in the flavonoid biosynthesis pathway, and hydroxyisoflavanone synthase (*Araip.0P3RJ*) and isoflavone 2'-hydroxylase (*Araip.S5EJ7*) in the isoflavonoid biosynthesis pathway were significantly upregulated by *AhHDA1* overexpression, while their expression in *AhHDA1-RNAi* and control hairy roots remained at a lower level or was unchanged. Our results suggest that alteration of secondary

 doi:10.20944/preprints201809.0486.v1

metabolism activities is related to overexpression of AhHDA1, which is mainly reflected in phenylpropanoid, flavonoid and flavonoid biosynthesis. Future studies will focus on the function of AhHDA1 interacting proteins and their action on cell growth and stress responses.

Keywords: Histone deacetylase, metabolism, peanut, hairy roots, RNA-seq

1. Introduction

During the various stages of development and in response to abiotic stresses, plant cells regulate the expression of many genes (Gan, et al., 2013; Lee, et al., 2015). Chromatin structure plays a key role in transcriptional regulation and is controlled by multiprotein complexes that recognize and instigate biochemical modifications of the histone proteins (Chen and Wu, 2015; Ganai, et al., 2016). Together, these multiprotein complexes, of which the core catalyzing enzymes are histone acetyltransferase proteins (HATs) and histone deacetylases (HDACs), maintain chromatin structure in a state of dynamic equilibrium (Mikkelsen et al., 2007). Thus, gene transcription can be activated by HATs through acetylation of lysine residues in the N-termini of histones H3 and H4, which switches the associated chromatin from a compacted to a looser state. In contrast, HDACs function as antagonists of HATs by removing acetyl groups from histone acetylation sites, resulting in transcriptional repression and gene silencing (Xing and Poirier, 2012; Ma et al., 2013). The fluctuating balance between HAT and HDAC activity comprises a large part of the epigenetic regulation of the genome; for example, recent evidence has revealed that regulation of histone acetylation plays a pivotal role in plant responses to salinity, drought and other stresses (Kim

et al., 2015).

HDACs have been isolated or identified in several plants and are well conserved across species, including Arabidopsis, rice, maize, grapevine and peanut (*Arachis hypogaea*) (Pandey et al., 2002; Ding et al., 2012; Yang et al., 2016; Aquea et al., 2010; Su et al.; 2015). Phylogenetic analysis has classified HDACs into three distinct families, namely RPD3/HDA1-like HDACs, SIR2-like HDACs, and HD2 proteins, based on sequence similarity, substrate specificity, and cofactor requirement (Ma et al., 2013; Bourque et al., 2016). The majority of the HDACs in a given plant species are of the RPD3/HDA1-like category; for example, *Arabidopsis thaliana* has 12 RPD3/HDA1 subfamily genes among 18 putative HDAC family genes (Ma et al., 2013). It has been reported that HDACs function in plant growth, development, stress responses and gene silencing, and are also involved in other cellular processes such as cell death and the cell cycle. HDA6, HDA9 and HDA19 are the most-studied HDACs. Thus, HDA6 features in the responses to various plant hormones: it not only participates in jasmonic acid (JA)- and abscisic acid (ABA)-mediated plant defense responses, but is also involved in transgene silencing-related auxin responses; furthermore, recently the *hda6* mutant was found to display a brassinosteroid (BR)-repressed phenotype in the dark and was less sensitive to BR biosynthesis inhibitors (Murfett et al., 2001; Devoto et al., 2002; Tanaka et al., 2008; Luo et al., 2012; Hao et al., 2016). HDA19 is involved in JA and ethylene signaling during the response to pathogens, and redundantly with *HDA6* regulates the repression of embryonic properties during germination (Zhou et al., 2005; Tanaka et al., 2008). *HDA9*, which acts to oppose the effect of its homologs HDA6 and HDA19, is a negative regulator of germination in seedlings: *hda9* mutant strains display

 doi:10.20944/preprints201809.0486.v1

reduced seed dormancy and faster germination than wild-type plants (van Zanten et al., 2014). Other HDACs have mostly been reported to have a role in plant growth and development. For instance, HDA5 interacts with FVE, FLD (FLOWERING LOCUS D) and HDA6, forming a protein complex involved in the regulation of flowering time (Luo et al., 2015); both overexpression and silencing of HDA7 lead to a delay in growth at postgermination and later developmental stages, while downregulation of HDA7 decreases silique fertility in Arabidopsis (Cigliano et al., 2013); by regulating kinase genes, HDA18 is involved in positional information signaling during cellular patterning of Arabidopsis root epidermis (Liu et al., 2013).

From the above, it is clear that HDAs are important in plant growth and development, and are key players in signal transduction responses to plant hormones. Accordingly, the regulation of histone acetylation provides a new perspective in crop breeding research. However, in many important crop plants, such as peanut, research on the epigenetic regulation of development and growth has rarely been reported and the mechanisms of these processes are not well understood. Others have reported that the peanut allergy gene *Ara h 3* undergoes an increase in histone H3 acetylation and a decrease in histone H3K9 dimethylation in embryos at an early stage of maturation (Fu et al., 2010), while histone deacetylation modification participates in the repression of peanut seed storage protein gene *Ara h 2.02* during germination (Yang et al., 2015). In our previous study, we isolated and characterized *AhHDA1* from *A. hypogaea*, showing that AhHDA1 is very similar in structure to an Arabidopsis HDAC (AtHDA6) and, in recombinant form, possesses HDAC activity (Su et al., 2015). We also found that *AhHDA1* is significantly upregulated by water deficit and

Preprints (www.preprints.org) | NOT PEER-REVIEWED | Posted: 25 September 2018 doi:10.20944/preprints201809.0486.v1

100 μM ABA. However, whether this HDAC mediates cell growth and development in peanut is not clear.

In this paper, we show that modifications in *AhHDA1* expression, particularly overexpression, have a significant morphological effect on hairy root cells. Furthermore, tsranscriptome sequencing suggests that *AhHDA1* regulates the biosynthesis of various carbon-mebolism-related biological molecules. These results provide insight into the role of AhHDA1 in peanut hairy roots, and lay the foundations for a wider understanding of histone deacetylase function in peanut, with potential impact on the breeding of new varieties.

2. Results

2.1. Overexpression of *AhHDA1* in transgenic hairy roots retards growth

35S::AhHDA1-eGFP (denoted *35S::AhHDA1* in the main text) and *35S::AhHDA1-RNAi* transgenic hairy roots were obtained by transforming four-leaf peanut seedlings. We observed that *35S::AhHDA1-eGFP* transgenic hairy roots became denser, with a dark coloration, after 20 d *in vitro* cultivation (Fig 1A and 1B). As the growth period progressed beyond 20 d, the *35S::AhHDA1-eGFP* transgenic hairy roots grew more slowly and eventually stopped growing entirely. In contrast, both *35S::AhHDA1-RNAi* and the control group maintained a relatively high growth rate, with the growth rate of *AhHDA1-RNAi* transgenic hairy roots being the highest (Fig 1C).

Preprints (www.preprints.org) | NOT PEER-REVIEWED | Posted: 25 September 2018 doi:10.20944/preprints201809.0486.v1

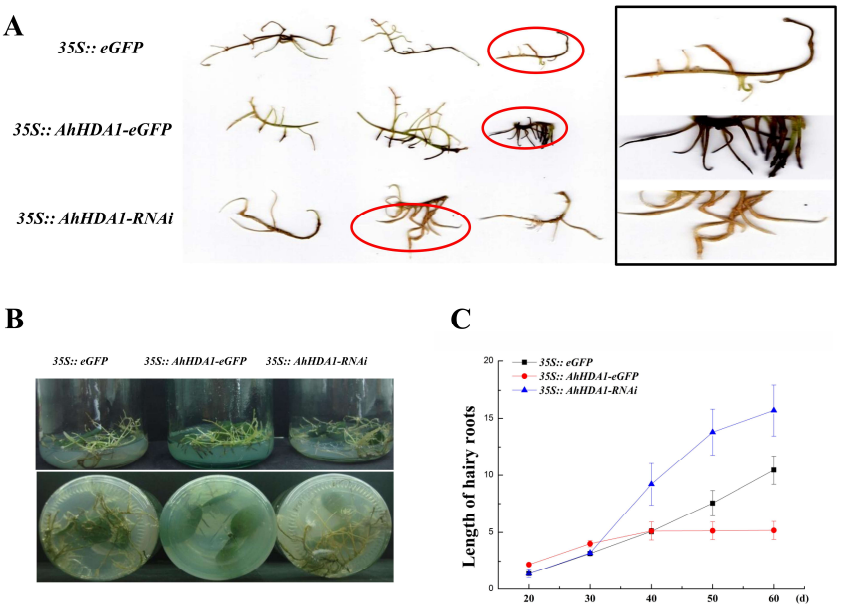

Fig 1. *35S::AhHDA1* transgenic hairy roots possess the characteristic of retarded growth. A. Growth morphology of the different transgenic hairy roots. B. The growing status of different transgenic hairy roots in *in vitro* cultivation. C. Growth rate of transgenic hairy roots, the values are the means of at least 50 replicates with standard deviation.

Under the light microscope, the cells at the surface of 15 d-cultivated overexpressing transgenic hairy roots appeared thick and indistinct, with less root hair in the hairy zone than the control group and the RNA interference group. Treatment with 20% PEG seemed to exacerbate this phenotype further (Fig 2A). Although there was no significant difference in cell size among the different groups in the meristem and near elongation regions, the hairy root cells overexpressing *AhHDA1* were significantly smaller than controls and the *35S::AhHDA1-RNAi* group in the root hair and far elongation regions (Fig 2B). Furthermore, the cell width-to-length ratios in *35S::AhHDA1* and *35S::AhHDA1-RNAi* transgenic hairy roots were smaller than controls, presenting as a long, narrow cell form. Thus, altered expression of *AhHDA1* had a clear effect on the morphology of cells near the root hair region (Fig 2B and Fig 2C).

Preprints (www.preprints.org) | NOT PEER-REVIEWED | Posted: 25 September 2018 doi:10.20944/preprints201809.0486.v1

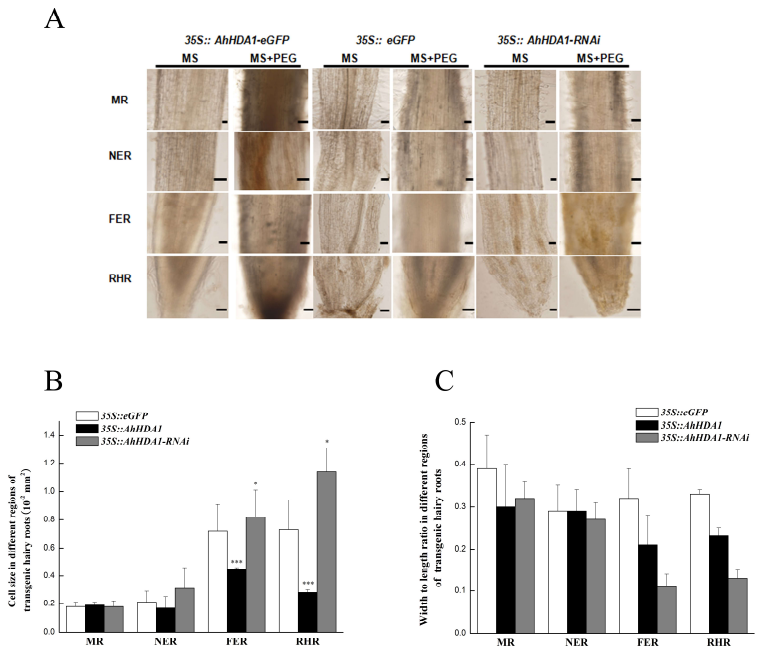

Fig 2. Morphologic observation of different transgenic peanut hairy roots with or without PEG treatment. A. Apical microscopic observation of transgenic hairy root (Black solid line displays the distance of 50 μM; MR: meristem region; NER: The near elongation region; FER: The far elongation region; RHR: Root hair region). B. Cell size in different regions of transgenic hairy roots. C. Width to length ratio in different regions of transgenic hairy roots.

The intracellular ROS concentration reflects the extent to which cells are experiencing environmental stress. We measured the relative concentration of superoxide anions and H_2O_2 in transgenic hairy roots using specific fluorescent probes. The superoxide anion concentration in 15 d overexpressed *AhHDA1* hairy roots was 4.06 times that of the blank control, while in the *35S::AhHDA1-RNAi* group it was 0.75 times that of controls. Similarly, the H_2O_2 concentration in overexpressed *AhHDA1* hairy roots was 2.81 times blank control levels, while in the *35S::AhHDA1-RNAi* group it was 0.77 times that of controls (Fig 3). Taken together with their abnormal phenotype and morphology, the increase in ROS level of *35S::AhHDA1* transgenic hairy roots suggests they are experiencing cell damage during this early growth stage.

Preprints (www.preprints.org) | NOT PEER-REVIEWED | Posted: 25 September 2018 doi:10.20944/preprints201809.0486.v1

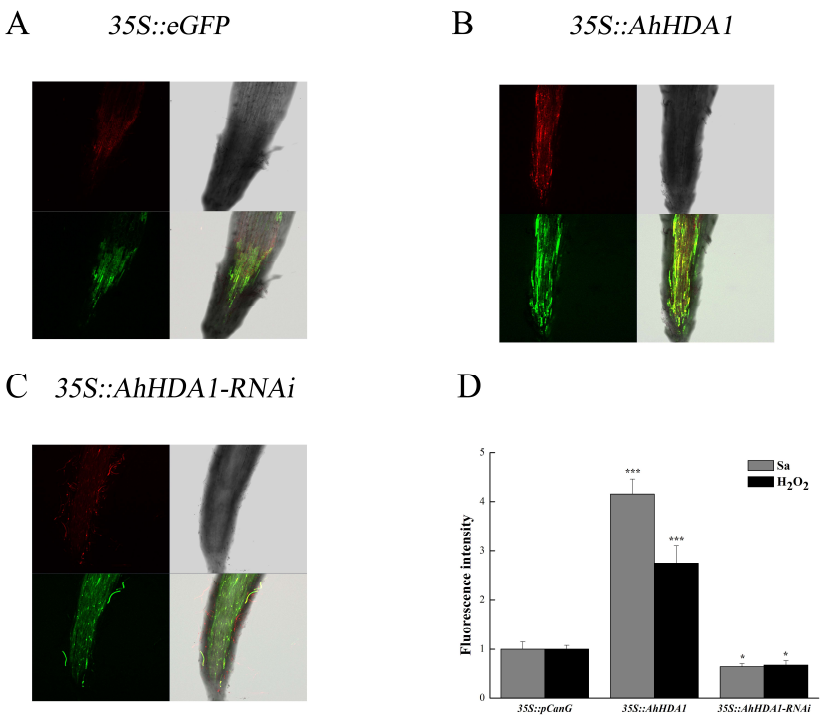

Fig 3. Reactive oxygen species have higher degree of accumulation in over-expressing *AhHDA1*(Red fluorescence represents super oxygen anion strength, Green fluorescence represents hydrogen peroxide content). A. Reactive oxygen species in *35S:: eGFP* transgenic hairy roots. B. Reactive oxygen species in *35S:: AhHDA1-eGFP* transgenic hairy roots. C. Reactive oxygen species in *35S:: AhHDA1-RNAi* transgenic hairy roots.

2.2. *AhHDA1* overexpression in hairy roots influences expression of biomolecular synthesis and metabolism genes

To investigate how *AhHDA1* affects cell morphology in hairy roots, we obtained transcriptome data for both *35S::AhHDA1* and *35S::AhHDA1-RNAi* hairy roots (www.ncbi.nlm.nih.gov/Traces/study/?acc=SRP113568) and compared these separately to the control group to identify differentially expressed genes (DEGs). Using criteria of >2-fold difference in expression level and $p<0.05$, we found 2157 DEGs by comparing the RPKM in different groups, and these were first subjected to GO enrichment classification (Fig 4). Most

 doi:10.20944/preprints201809.0486.v1

DEGs influenced by AhHDA1 could be grouped under the categories of cell part, membrane and intracellular in cellular component (166, 154 and 148 genes respectively), binding (824 genes) and catalytic activity (574 genes) in molecular function, metabolic process (637 genes), oxidation-reduction process (179 genes) in biological process. It is worth noting that in the category of biological process, relatively large numbers of genes could also be grouped under response to stimulus, protein modification process and transport, i.e. respectively, 144, 131 and 130 genes.

Preprints (www.preprints.org) | NOT PEER-REVIEWED | Posted: 25 September 2018 doi:10.20944/preprints201809.0486.v1

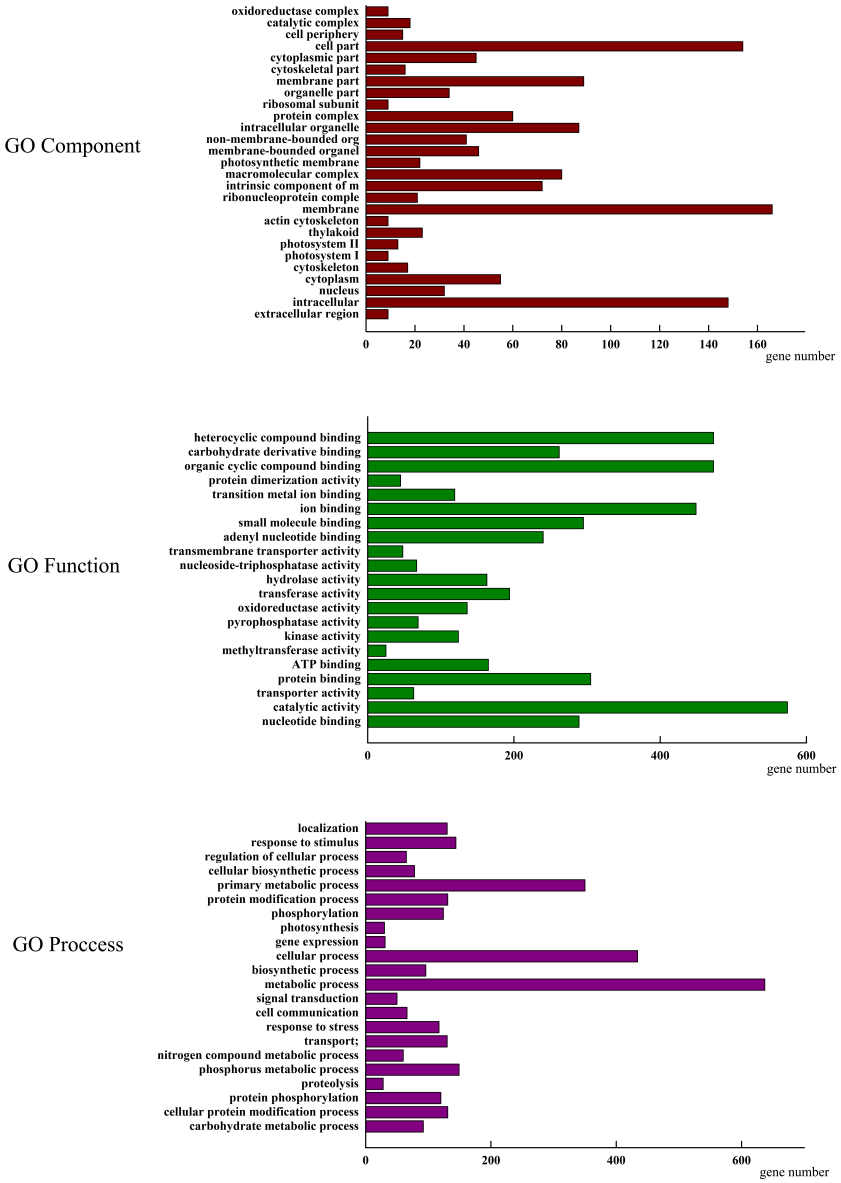

Fig 4. GO enrichment of DEGs among the control group, *35S:: AhHDA1* and *35S::AhHDA1-RNAi* hairy roots. Fourty GO terms were identified in the three root terms: biological process (BP), cellular component (CC) and molecular function (MF).

To obtain a deeper understanding of the role of the DEGs identified, we examined the pathways in which their gene products are thought to operate. Unfortunately, most DEGs could not be found in the Kyoto Encyclopedia of Genes and Genomes (KEGG) database because relatively few peanut genes and proteins have been annotated, but 468 out of the total

 doi:10.20944/preprints201809.0486.v1

of 2157 DEGs could be assigned to a KEGG pathway (Fig 5). We found the starch and sucrose metabolism (ko00500), carbon metablism (ko01200) and photosynthesis pathways (ko00195) to be the most gene-enriched pathways with 41, 33 and 31 genes, respectively. Other pathways, including phenylpropanoid biosynthesis (ko00940), oxidative phosphorylation (ko00190), plant hormone signal transduction (ko04075) and isoflavonoid biosynthesis (ko00943) pathways, were also indicated as modulated by AhHDA1 through its effect on the expression of downstream genes (Table S1). Of those annotated, 31 DEGs were identified as the most significantly differentially expressed, and 25 of these were found to be associated with biosynthesis and metabolism (Table 1). This result suggests that AhHDA1 influences several biosynthetic and metabolic pathways. In the starch and sucrose metabolism pathway, 12 beta-glucosidases and 5 trehalose-6-phosphate phosphatases were found to be differentially expressed: in *35S::AhHDA1* transgenic hairy roots, most of these genes were downregulated, while in the *35S::AhHDA1-RNAi* group expression of these genes remained unchanged or was upregulated (Fig S1). In the biomolecular synthesis pathways identified (which include phenylpropanoid biosynthesis, isoflavonoid and flavonoid biosynthesis, diterpenoid biosynthesis, and plant hormone biosynthesis, among others), 43 DEGs were upregulated and 78 DEGs were downregulated in *35S::AhHDA1* transgenic hairy roots (Fig S2). At the same time, six DEGs were downregulated and nine DEGs were upregulated in the *35S::AhHDA1* group in 19 DEGs, which were related with auxin (IAA), abscisic acid (ABA) and methyl jasmonate (MeJA) (Fig S3). In the photosynthesis pathway, 49 DEGs were downregulated in hairy roots overexpressing *AhHDA1*, with most DEGs remaining unchanged or being upregulated (Fig S4). These results imply that overexpression of

Preprints (www.preprints.org) | NOT PEER-REVIEWED | Posted: 25 September 2018 doi:10.20944/preprints201809.0486.v1

AhHDA1 in peanut hairy roots directs a slowdown of the cell's primary metabolic activity, while promoting secondary metabolic activity.

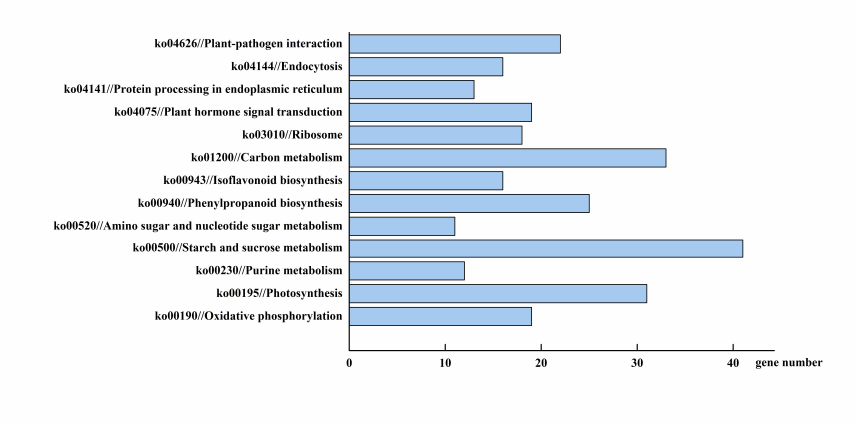

Fig 5. KEGG pathway AhHDA1 influenced DEGs annotation.

Table 1. The most significant differential expressed genes AhHDA1 influenced.

id	Ck-fpkm	H-fpkm	R-fpkm	Description	KEGG_B_class
Aradu.65YXV	1.035	8.675	6.9	polygalacturonase 4	Carbohydrate metabolism
Aradu.CPP65	0.11	0.075	0.005	helicases; nucleic acid binding;DNA binding	Transcription
Aradu.E1U58	0.12	0.225	0.67	pyruvate phosphate dikinase	Energy metabolism;Carbohydrate metabolism
Aradu.F5K8Q	0.34	1.225	2.835	alpha carbonic anhydrase 7	Energy metabolism
Aradu.G6ZA5	0.44	0.605	2.25	heat shock protein 70	Folding, sorting and degradation
Aradu.GP6IB	0.565	9.985	3.04	cinnamyl alcohol dehydrogenase 9	Biosynthesis of other secondary metabolites
Aradu.I3YXT	3.955	0.185	5.15	Glucose-methanol-choline	Lipid metabolism
Aradu.J6XSM	11.965	372.715	10.585	chalcone synthase	Biosynthesis of other secondary metabolites;Environmental adaptation
Aradu.KD6QW	42.25	9.85	2.485	HXXXD-type acyl-transferase family protein	Lipid metabolism
Aradu.KH972	5.155	6.16	0.31	beta glucosidase 17	Carbohydrate metabolism;Metabolism of other amino acids;Biosynthesis of other secondary metabolites
Aradu.M62BY	14.27	306.14	67.96	caffeoyl-CoA 3-O-methyltransferase	Biosynthesis of other secondary metabolites;Amino acid metabolism
Aradu.MI3AU	1.58	137.715	4.09	Cytochrome P450 superfamily protein	Biosynthesis of other secondary metabolites
Aradu.MZ55S	5.36	0.35	3.36	NAD(P)H-quinone oxidoreductase subunit H	Energy metabolism
Aradu.NB8XZ	0.04	0.94	0.21	beta-fructofuranosidase 5	Carbohydrate metabolism
Aradu.NL8HQ	0.095	0.085	0.65	heat shock protein 21	Folding, sorting and degradation
Aradu.R479P	2.02	0.095	1.105	gamma-tocopherol methyltransferase	Metabolism of cofactors and vitamins
Aradu.SK1BS	9.755	4	0.485	seed linoleate 9S-lipoxygenase	Lipid metabolism
Aradu.X1FHB	0.565	0.66	0.03	mannan endo-1,4-beta-mannosidase 6-like	Carbohydrate metabolism
Araip.0P3RJ	12.56	336.055	34.235	Cytochrome P450 superfamily protein	Biosynthesis of other secondary metabolites
Araip.2J996	0.43	0.02	0.37	Disease resistance protein (TIR-NBS-LRR class)	Environmental adaptation

 doi:10.20944/preprints201809.0486.v1

Araip.57AWT	1.555	0.04	0.855	1-aminocyclopropane-1-carboxylate synthase 11	Amino acid metabolism
Araip.645JG	0.48	0.025	0.05	phosphoinositide phospholipase C 2-like	Signal transduction;Carbohydrate metabolism
Araip.68IEK	1.06	0.05	0.735	prephenate dehydrogenase family protein	Amino acid metabolism
Araip.99LMI	1.53	0.09	0.38	cyclic nucleotide-gated ion channel-like protein	Environmental adaptation
Araip.B8TJ0	8.21	742.68	15.78	chalcone synthase	Biosynthesis of other secondary metabolites;Environmental adaptation
Araip.F9GZL	0.205	8.17	0.695	Glycosyltransferase family 29 (sialyltransferase)	Glycan biosynthesis and metabolism
Araip.G4SZ0	0.575	10.785	0.715	myo-inositol oxygenase 2	Carbohydrate metabolism
Araip.H9S11	0.65	0.145	0.045	ent-copalyl diphosphate synthase, chloroplastic-like isoform X3	Metabolism of terpenoids and polyketides
Araip.I4FSL	1.08	0.735	0.05	putative indole-3-acetic acid-amido synthetase	Signal transduction
Araip.IUY1V	0.19	4.79	1.61	cinnamyl alcohol dehydrogenase 6	Biosynthesis of other secondary metabolites
Araip.K461S	3.52	9.69	0.115	1-deoxy-D-xylulose 5-phosphate synthase 1	Metabolism of terpenoids and polyketides;Metabolism of cofactors and vitamins

To verify the transcriptome results, six DEGs thought to be important in biomolecular synthesis-related pathways were selected and their expression determined by real time-PCR (RT-PCR): *Araip.XGB85* (caffeoyl-CoA O-methyltransferase, CCoAOMT) and *Araip.Z3XZX* (caffeic acid 3-O-methyltransferase) in the phenylpropanoid biosynthesis pathway, *Araip.B8TJ0* (chalcone synthase, CHS) and *Araip.MKZ27* (polyketide reductase) in the flavonoid biosynthesis pathway, and *Araip.0P3RJ* (hydroxyisoflavanone synthase) and *Araip.S5EJ7* (isoflavone 2'-hydroxylase) in the isoflavonoid biosynthesis pathway. The transcriptional levels of these six DEGs in the *35S::AhHDA1* transgenic group were found to be significantly higher than in the control and *35S::AhHDA1*-RNAi groups (Fig 6). This is consistent with the transcriptome data. Together, these results indicate that overexpression of *AhHDA1* enhances the transcriptional level of phenylpropanoid, flavonoid and flavonoid biosynthesis genes, all of which are involved in secondary metabolism. The higher expression levels of these genes might be related to the slower growth rates in these transgenic plants.

Preprints (www.preprints.org) | NOT PEER-REVIEWED | Posted: 25 September 2018 doi:10.20944/preprints201809.0486.v1

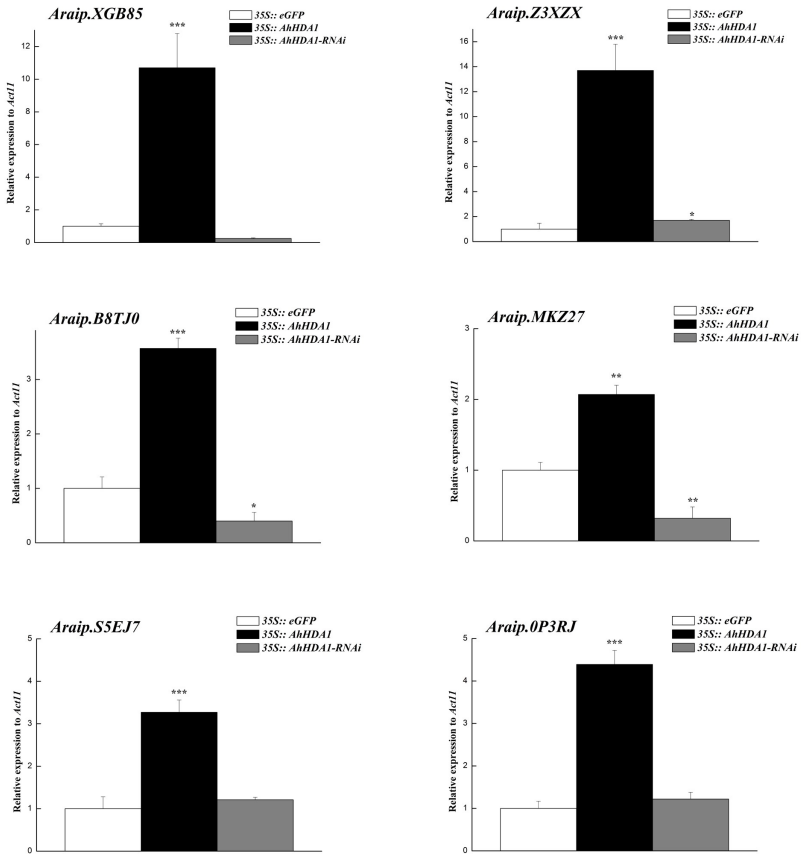

Fig 6. Transcript levels measured by real-time RT-qPCR in different transgenic hairy roots (*Araip.XGB85*, Caffeoyl-CoA O-methyltransferase; *Araip.Z3XZX*, Caffeic acid 3-O-methyltransferase; *Araip.B8TJ0*, chalcone synthase; *Araip.MKZ27*, Polyketide reductase; *Araip.0P3RJ*, Hydroxyisoflavanone synthase; *Araip.S5EJ7*, Isoflavone 2'-hydroxylase). *Act11* was used as an internal control. Results from experiments repeated three times, each with three qPCR measurements, indicating the mean±SEM, n= 3 replicates (6–8 plants were pooled for each measurement). Each graph displays the mean and SD of three independent experiments. */**, different from control as revealed by *t*-test, $p<0.05/0.01$.

3. Discussion

Peanut (*Arachis hypogaea* L.), as a source of edible oil and protein, is one of the most economically important crops, the seed oil content of which can reach 45-56% (Chen et al., 2016). Thus, the growth and developmental characteristics of peanut are of considerable interest. We have chosen to examine the role of epigenetics in peanut growth and development because this field is underinvestigated in crop plants, although there have been

 doi:10.20944/preprints201809.0486.v1

many in-depth studies in model plant species, where, for example, HDAC activity has been implicated in plant growth, cell development, hormone responses and the response to environmental stress (Yu et al., 2011; Luo et al., 2012; Perrella et al., 2013; Hao et al., 2016; Zheng et al., 2016).

3.1. Overexpression of AhHDA1 increases expression of phenylpropanoid secondary metabolic pathway genes

In earlier studies, peanut *AhHDA1* was isolated and was found to be induced by ABA and PEG (Su et al., 2015). In the current study, we investigated the role of *AhHDA1* in more detail and observed that overexpression of causes retarded growth during the early growth of hairy roots (Fig 1). Under the light microscope, significant changes in cell morphology were observed near the root hair region in these overexpressing plants, with the cell size being significantly smaller than in other groups. Moreover, the width-to-length ratios of hairy root cells in both the overexpressing and RNA interference groups were smaller than in controls, with cells near the root hair region being long and narrow in shape (Fig 2). Transcriptome sequencing was carried out to improve our understanding of how *AhHDA1* might mediate this alteration in cell morphology. We found that pathways involved with various aspects of metabolism, biomolecular biosynthesis and photosynthesis were significantly influenced by *AhHDA1* (Fig S1). Thus, 131 DEGs were downregulated and 58 DEGs were upregulated in various metabolic pathways, with the starch and sucrose metabolism, and carbon metabolism pathways containing the most DEGs (Fig S1). In particular, nine DEGs in the isoflavonoid biosynthesis pathway (five cytochrome P450 superfamily proteins and four

 doi:10.20944/preprints201809.0486.v1

O-methyltransferase family proteins) were upregulated and seven DEGs in the isoflavonoid biosynthesis pathway (six O-methyltransferase family proteins and one cytochrome P450 superfamily protein) were downregulated. In the phenylpropanoid biosynthesis pathway, 13 DEGs (including four cinnamyl alcohol dehydrogenase and four peroxidase superfamily proteins) were downregulated, while 11 DEGs in the phenylpropanoid biosynthesis pathway (including nine peroxidase superfamily proteins) were upregulated (Fig S2). The most remarkable finding was that overexpression of *AhHDA1* changed the expression pattern of all 49 DEGs relating to photosynthesis and oxidative phosphorylation, although most of these DEGs were unaffected in *AhHDA1-RNAi* hairy roots.

The phenylpropanoid secondary metabolic pathway influences many important plant traits through the synthesis of a large number of secondary metabolites such as lignins and flavonoids (Le et al., 2016). The biosynthesis of lignin precursors proceeds through the phenylpropanoid pathway leading to the synthesis of cinnamoyl-CoA esters. CCoAOMTs play an important role in lignin biosynthesis and the promoters of CCoAOMT genes are responsive to signals that control lignin deposition throughout plant development, thereby adjusting lignin quality in response to environmental conditions (Chen et al., 2000; Zhong et al., 2000). At the same time, the flavonoid and isoflavonoid synthesis pathways connect with the phenylpropanoid pathway and thus with lignin synthesis. Experiments in *A. thaliana* show that, in hydroxycinnamoyl-CoA shikimate/quinate hydroxycinnamoyl transferase (HCT)-silenced plants, repression of lignin synthesis leads to the redirection of the metabolic flux into flavonoids through chalcone synthase activity (Besseau et al., 2007). Furthermore, coordinated regulation of genes involved in flavonoid metabolism can redirect flux into the

 doi:10.20944/preprints201809.0486.v1

isoflavonoid branch of the phenylpropanoid pathway, by reducing competition for the flavanone substrate. The experimental results, which showed good reproducibility, were also validated by principal component analysis of the gene transcript data (Fig. S5). Based on this, our experiments demonstrate that *AhHDA1* overexpression causes retarded growth of transgenic hairy roots, and is associated with increased expression of phenylpropanoid secondary metabolic pathway genes (Fig 6). It is clear that the expression of these secondary metabolite synthesis genes is relevant to *AhHDA1* differential expression.

3.2. AhHDA1 interacting proteins and their potential biological functions

From the experimental results, AhHDA1 seems to be involved in peanut hairy root growth and development, particularly in respect of the phenylpropanoid secondary metabolic pathway. However, the molecular details of how AhHDA1 influences this metabolic pathway are currently unclear. For an in-depth understanding of the downstream genes influenced by AhHDA1, it will be important to know which proteins interact with it and to identify their functions. In Arabidopsis, researchers have screened for RPD3/HDA1 family-interacting proteins, and these interacting proteins are involved in plant organogenesis, development and stress responses. For example, orchestrated repression of SEP3 by Short Vegetative Phase (SVP), Agamous-Like 24 (AGL24), and Suppressor of Overexpression of Constans 1 (SOC1) is mediated by recruiting SAP18, a member of the SIN3 HDAC complex, which influences floral patterning (Liu et al., 2009). In another example, HDA15 was found to interact directly with PIF3 and NF-YCs in vivo and in vitro. PIF3 targets the genes involved in photosynthesis and chlorophyll biosynthesis in the dark and represses gene expression, while NF-YCs

 doi:10.20944/preprints201809.0486.v1

function as transcriptional co-repressors by interacting with HDA15 to inhibit hypocotyl elongation in photomorphogenesis during the early seedling stage (Liu et al., 2013; Tang et al., 2017). Other researchers also reported that HDA-interacting proteins are involved in stress responses. Thus, the cold signaling attenuator High Expression of Osmotically Responsive Gene1 (HOS1) negatively regulates cold responses by interacting with its interacting partner histone deacetylase 6 (HDA6) under short-term cold stress (Jung et al., 2013). In wheat, FVE/MSI4 is a WD-40 repeat-containing protein that can form the FAE-HAD6-FLD complex, which plays important roles in co-regulating gene expression in multiple developmental processes including flowering time and abiotic stress (Yu et al., 2016; Zheng et al., 2017). From the above, it is clear that RPD3/HDA1 family proteins are involved in cell development and stress responses.

Using the yeast two-hybrid technique, 37 AhHDA1-interacting protein candidates were identified (Table S2). Some of the most interesting proteins that interacted with AhHDA1 are APRR2-like, GLK1-like, bHLH77-like, NAC2 and MYB-like transcription factors. Three molecular chaperones or their regulators were also found, and these may function in nucleosome assembly. In addition to these examples, 18 proteins might be involved in cellular synthetic metabolic pathways, while nine proteins are related to stress responses and six proteins to photosynthesis and oxidative phosphorylation. Although these candidate interacting proteins require further experimental analysis, they potentially provide insight into how AhHDA1 might regulate synthetic metabolic pathways, cellular defense responses, and photosynthesis and oxidative phosphorylation via the proteins it interacts with.

In this study, differential expression of AhHDA6, which is a RPD3/HDA1 subfamily

 doi:10.20944/preprints201809.0486.v1

member, was shown to modify cell morphogenesis and developmental in peanut hairy roots and to retard cell growth (Fig 1 and Fig 2). Transcriptome analysis implicated certain synthetic metabolic pathways in the cause of the observed phenotype. Few similar results have been reported previously in other plants, perhaps because *AhHDA1* possesses different features to RPD3/HDA1 genes in other species, or because the phenomenon of HDAC-inhibited cell growth is stage- and/or tissue-specific. In future studies, AhHDA1-interacting proteins will be identified and studied in detail, which will provide further insight into the molecular mechanisms of AhHDA1 function and its role in cell growth and development in hairy roots, thereby possibly laying the foundations for improvements in crop plant varieties.

4. Material and Methods

4.1. Plant materials and growth conditions

Seeds of peanut (*Arachis hypogaea* L. cv Yueyou 7) (Fang et al., 2007) were sown in pots with a potting mixture of vermiculite, perlite and soil (1: 1: 1), and grown in an illuminated incubator with 16 h of light from fluorescent and incandescent lamps (200 μmol m^{-2} s^{-1}) at 26˚C followed by 8 h of darkness at 22˚C. Plants were watered with half-strength Murashige and Skoog nutrient solution every other day (Su et al., 2015).

4.2. Agrobacterium strain and binary vector

The cucumopine-type *A. rhizogenes* strain K599 was used to induce transgenic hairy roots in peanut. The AhHDA1 cassette was released from pCanG-AhHDA1, which was previously constructed by the pCanG-vector to form the overexpressing AhHDA1 recombinant plasmid,

Preprints (www.preprints.org) | NOT PEER-REVIEWED | Posted: 25 September 2018 doi:10.20944/preprints201809.0486.v1

under the control of the cauliflower mosaic virus (CaMV) 35S promoter. The AhHDA1 interference recombinant plasmid also used pCanG as the construct backbone. The 542 bp sense sequence was chosen, and the primer sequences were designed as forward (AhHDA1-sense-F: 5'-ccgctcgagGACGTTGGTGTTGGCTCAGG-3') and reverse (AhHDA1-sense-R: 5'-cccaagcttCTCTCCATGTCCTCTTCTGCC-3'). Antisense primer sequences were designed as forward (AhHDA1-antisense-F: 5'-CGAGCTCCTCTCCATGTCCTCTTCTGCC-3') and reverse (AhHDA1-antisense-R: 5'-CTAGACTAGTGACGTTGGTGTTGGCTCAGG-3'). The resulting binary constructs *35S::AhHDA1-eGFP* and *35S::AhHDA1-RNAi*, together with the original plasmid *35S::eGFP*, were separately transformed into the K599 strain. The neomycin phosphotransferase gene (NPTII), under the control of the nopaline synthase (NOS) promoter located within T-DNA enabled positive transformants to be selected by kanamycin. Peanut hairy root induction resulted in transgenic hairy root formation (Liu et al., 2016b).

4.3. Yeast two-hybrid analysis

After treated by 30% PEG6000 (W/V) for 5 h, total RNA in peanut roots, stems and leaves were extracted to construct yeast cDNA library. The cDNA fragments were ligated to pGADT7 plasmid and stored in yeast cells. Full length *AhHDA1* cDNA was amplified by PCR using the following primer pairs: AhHDA1-EcoR1-F: 5'-TACGAATTCATGGGGATA GAAGAAGAGAG-3', AhHDA1-Sac1-R: GAGCTCTCAGCAGCATCCATGTGG-3'. The PCR fragment was ligated into the vector pGBKT7 (Clontech, USA) after cleavage by restriction endonucleases *Eco*RI and *Sac*I (New England Biolabs, USA). pGBKT7-AhHDA1 and the yeast library plasmid were co-transformed to AH109 competent cells. After

 doi:10.20944/preprints201809.0486.v1

screened on the SD/Trp^{-}/Leu^{-}/His^{-} selective medium, all fragments cloned were checked by PCR and sequenced. The two-hybrid assays were performed using the Matchmaker^{TM} Gold two-hybrid system (Clontech) following the manufacturer's protocols (Liu et al., 2016a).

4.4. Measurements of intracellular reactive oxygen species

A superoxide anion chemiluminescent probe (Wako, Cat No. 075-05111) and a BES-H_2O_2-Ac H_2O_2 probe (Wako, Cat No. 028-17811) were used to measure superoxide anion content and H_2O_2 content, respectively, which reflect the levels of intracellular reactive oxygen species (ROS) (Kawase et al., 2004; Teranishi et al., 2007). After washing with phosphate-buffered saline, hairy root tips were soaked with BES-H_2O_2-Ac fluorescence probe and superoxide anion chemiluminescent probe for 20 min and imaged using a laser scanning confocal microscope (Leica TCS SP8) (Yamamoto et al., 2017). Then the samples were ground and homogenized in phosphate buffer solution (pH7.4), and the supernatant was collected after centrifugation. Plate-reader-based luminescence measurements were performed in 96-well plates using a multimode reader (Molecular Devices, SpectraMax M5; wavelengths 488 nm and 610 nm, respectively), with temperature set at 37˚C.

4.5. RNAseq and data analysis

After 20 d growth, *35S::eGFP, 35S::AhHDA1-eGFP* and *35S::AhHDA1-RNAi* transgenic hairy roots were collected from at least 10 different hairy roots that comes from different sites of hairy roots, as independent biological replicates for transcriptome analysis. Total RNA in every sample was no less than 5 μg. The total RNA samples were first treated with DNase I (NEB, Cat. No. M0303) to degrade any contaminating DNA. Then the samples were enriched for mRNA using oligo(dT) magnetic beads (NEB, Cat. No. S1419). After mixing with

 doi:10.20944/preprints201809.0486.v1

fragmentation buffer, the mRNA was broken into short fragments (about 200 bp). Then first-strand cDNA was synthesized using random hexamer primers (NEB, Cat. No. E7771). Buffer, dNTPs, RNase H and DNA polymerase I were added to synthesize the second strand and double-stranded cDNA was purified with AMPure XP Beads (NEB, Cat. No. E7330). End repair and 3'-end single nucleotide A addition were then performed using the Next® Ultra™ II End Repair/dA-Tailing Module (NEB, Cat. No. E7546). Finally, sequencing adaptors were ligated to the fragments. The library products were sequenced on the Illumina Hiseq 2000 platform. Clean reads were obtained by removing reads containing adapter, reads containing polyN and low-quality reads from raw data, and were aligned to the peanut genome (http://peanutbase.org/home) using Soap (2.21) software (http://soap.genomics.org.cn/). The gene expression level was quantified using the RPKM method; the RPKM of each gene was calculated based on the length of the gene and the read count mapped to this gene. The genes' RPKM values were calculated based on all uniquely mapped reads. Differential expression analysis was implemented using the Poisson distribution model, and genes with a false discovery rate ≤ 0.001 and more than twice the difference between either the overexpressing AhHDA1 or the AhHDA1 interference group and the control group were assigned as differentially expressed (criteria of >2-fold difference in expression level and $p<0.05$).

4.6. Reverse transcription and real-time PCR

RNA extraction was carried out as described (Su et al., 2015). Three biological replicate RNA samples for each time point and treatment were used for downstream applications. Relative expression for each well was calculated (Muller et al., 2002). Expression data for *A.*

 doi:10.20944/preprints201809.0486.v1

hypogaea L. was normalized using the geometric mean (geomean) of the validated housekeeping gene, *ACTIN* (Chi et al., 2012): the primers ACT11-F (5'-GATTGGAATGGAAGCTGCTG-3') and ACT11-R (5'-CGGTCAGCAATACCAGGGAA-3'), specific to the peanut *ACTIN* gene (GenBank accession no. GO339334), were used to amplify a fragment of 108 bp. The mean values shown (±SE) were calculated from three biological replicates. The primers used for DEG expression verification are as follows: Araip.XGB85-F: 5'-AAAGGCTGGAGTAGAGCA-3', Araip.XGB85-R: 5'-TTCCCAAGTTTGAAG GAT-3'; Araip.Z3XZX-F: 5'-TGGTTGATGTAGGAGGTG-3', Araip.Z3XZX-R: 5'- GATATGATGGTGCGTTTT-3'; Araip.B8TJ0-F: 5'-CATGGTGGTTGTGGAGGT-3', Araip.B8TJ0-R: 5'-GCTGGTGGTGCAGAAGAT-3'; Araip.MKZ27-F: 5'-CAGGCA AGGCTACAGGCACT-3', Araip.MKZ27-R: 5'-AGAGGTCTTGGCGGGTGA-3'; Araip.S5EJ7-F: 5'-TGGAGGAGGCGAAGCAGT-3', Araip.S5EJ7-R: 5'-CCCAAGC AGCGGAATGAA-3'; Araip.0P3RJ-F: 5'-TGCTTGCTTCGCTCATTC-3', Araip.0P3RJ-R: 5'-GCCCTGTTATCCTTACCCT-3'.

 doi:10.20944/preprints201809.0486.v1

Abbreviations

AhHDA1: Peanut histone deacetylase 1

ABA: Abscisic acid

RNA-seq: RNA sequencing

RNAi: RNA interference

RT-PCR: Realtime PCR

HATs : Histone acetyltransferase proteins

HDACs : Histone deacetylases

JA : Jasmonic acid

BR: Brassinosteroid

ROS: Reactive oxygen species

DEGs: Differentially expressed genes

FDR: False discovery rate

Competing interests

The authors declare that they have no competing interests.

Authors' contributions

LCS, SL and LL designed and directed the research; LCS, BHZ and MJL analyzed the data; LCS wrote the manuscript with input from all authors; XL, BHZ, LDZ and LL contributed new techniques. All authors edited and agreed on the final manuscript.

Acknowledgements

This work was supported by grants from the National Natural Science Foundation of China (No. 31471422 granted to LL; No. 31860310 granted to LCS).

Reference

Aquea F, Timmermann T, Arce-Johnson P. Analysis of histone acetyltransferase and deacetylase families of *Vitis vinifera*. Plant Physiol Biochem. 2010; 48(2-3): 194-9. doi: 10.1016/j.plaphy.2009.12.009.

Besseau S, Hoffmann L, Geoffroy P, Lapierre C, Pollet B, Legrand M. Flavonoid accumulation in Arabidopsis repressed in lignin synthesis affects auxin transport and plant growth. Plant Cell. 2007; 19(1): 148-62. doi: 10.1105/tpc.106.044495.

Bourque S, Jeandroz S, Grandperret V, Lehotai N, Aime S, Soltis DE, . . . Nicolas-Frances V. The Evolution of HD2 Proteins in Green Plants. Trends Plant Sci. 2016; 21(12): 1008-16. doi: 10.1016/j.tplants.2016.10.001.

Chen C, Meyermans H, Burggraeve B, De Rycke RM, Inoue K, De Vleesschauwer V, Steenackers M, Van Montagu MC, Engler GJ, Boerjan WA. Cell-specific and conditional expression of caffeoyl-coenzyme A-3-O-methyltransferase in poplar. Plant Physiol. 2000; 123(3): 853-67.

Chen LT, Wu K. Role of histone deacetylases HDA6 and HDA19 in ABA and abiotic stress response. Plant Signal Behav. 2010; 5(10): 1318-20. doi: 10.4161/psb.5.10.13168.

Chen X, Li H, Pandey MK, Yang Q, Wang X, Garg V, … Yu S. Draft genome of the peanut A-genome progenitor (*Arachis duranensis*) provides insights into geocarpy, oil biosynthesis, and allergens. Proc Natl Acad Sci U S A. 2016; 113(24): 6785-90. doi: 10.1073/pnas.1600899113.

Chi X, Hu R, Yang Q, Zhang X, Pan L, Chen N, Yu S. Validation of reference genes for gene expression studies in peanut by quantitative real-time RT-PCR. Mol Genet Genomics.2012;

287(2): 167-76. doi: 10.1007/s00438-011-0665-5.

Cigliano RA, Cremona G, Paparo R, Termolino P, Perrella G, Gutzat R, . . . Conicella C. Histone deacetylase AtHDA7 is required for female gametophyte and embryo development in Arabidopsis. Plant Physiol. 2013; 163(1): 431-40. doi: 10.1104/pp.113.221713.

Devoto A, Nieto-Rostro M, Xie D, Ellis C, Harmston R, Patrick E, . . ., Turner JG. COI1 links jasmonate signalling and fertility to the SCF ubiquitin-ligase complex in Arabidopsis. Plant J. 2002; 32(4): 457-466. doi: 10.1046/j.1365-313X.2002.01432.x.

Ding B, Bellizzi MR, Ning Y, Meyers BC, Wang GL. HDT701, a histone H4 deacetylase, negatively regulates plant innate immunity by modulating histone H4 acetylation of defense-related genes in rice. Plant Cell. 2012; 24(9): 3783-94. doi: 10.1105/tpc.112.101972.

Fang XL, Liao WQ, Xiao LC, Zhou GY, Li DY, and Cai SH. A primary report on the introduction and demonstration of super high yield peanut variety Yueyou7. J. Peanut Sci. 2007; 36: 38–40. doi: 10.3969/j.issn.1002- 4093. 2007. 02. 009.

Fu G., Zhong Y, Li C, Li Y, Lin X, Liao B, . . . Huang S. Epigenetic regulation of peanut allergen gene *Ara h 3* in developing embryos. Planta. 2010; 231(5): 1049-60. doi: 10.1007/s00425-010-1111-3.

Gan ES, Huang J, Ito T. Functional roles of histone modification, chromatin remodeling and microRNAs in Arabidopsis flower development. Int Rev Cell Mol Biol. 2013; 305: 115-61. doi: 10.1016/B978-0-12-407695-2.00003-2.

Ganai SA, Banday S, Farooq Z, Altaf M. Modulating epigenetic HAT activity for reinstating acetylation homeostasis: A promising therapeutic strategy for neurological disorders.

Pharmacol Ther. 2016; 166: 106-22. doi: 10.1016/j.pharmthera.2016.07.001.

Hao Y, Wang H, Qiao S, Leng L, Wang X. Histone deacetylase HDA6 enhances brassinosteroid signaling by inhibiting the BIN2 kinase. Proc Natl Acad Sci U S A. 2016; 113(37): 10418-23. doi: 10.1073/pnas.1521363113.

Jung JH, Park JH, Lee S, To TK, Kim JM, Seki M, Park CM. The cold signaling attenuator HIGH EXPRESSION OF OSMOTICALLY RESPONSIVE GENE1 activates FLOWERING LOCUS C transcription via chromatin remodeling under short-term cold stress in Arabidopsis. Plant Cell. 2013; 25(11), 4378-90. doi: 10.1105/tpc.113.118364.

Kawase T, Fujiwara N, Tsutumi M, Oda M, Maeda Y, Wakahara T, Akasaka T. Supramolecular dynamics of cyclic [6]paraphenyleneacetylene complexes with [60]- and [70]fullerene derivatives: electronic and structural effects on complexation. Angew Chem Int Ed Engl. 2004; 43(38): 5060-2. doi: 10.1002/anie.200460630.

Kim JM, Sasaki T, Ueda M, Sako K, Seki M. Chromatin changes in response to drought, salinity, heat, and cold stresses in plants. Front Plant Sci. 2015; 6: 114. doi: 10.3389/fpls.2015.00114.

Le Roy J, Huss B, Creach A, Hawkins S, Neutelings G. Glycosylation Is a Major Regulator of Phenylpropanoid Availability and Biological Activity in Plants. Front Plant Sci. 2016; 7: 735. doi: 10.3389/fpls.2016.00735.

Lee K, Park OS, Jung SJ, Seo PJ. Histone deacetylation-mediated cellular dedifferentiation in Arabidopsis. J Plant Physiol. 2016; 191: 95-100. doi: 10.1016/j.jplph.2015.12.006.

Liu C, Li LC, Chen WQ, Chen X, Xu ZH, Bai SN. HDA18 affects cell fate in Arabidopsis root epidermis via histone acetylation at four kinase genes. Plant Cell. 2013; 25(1): 257-69.

doi: 10.1105/tpc.112.107045.

Liu C, Xi W, Shen L, Tan C, Yu H. Regulation of floral patterning by flowering time genes. Dev Cell. 2009; 16(5): 711-22. doi: 10.1016/j.devcel.2009.03.011.

Liu S, Li M, Su L, Ge K, Li L, Li X, . . . Li L. Negative feedback regulation of ABA biosynthesis in peanut (*Arachis hypogaea*): a transcription factor complex inhibits AhNCED1 expression during water stress. Sci Rep. 2016; 6: 37943. doi: 10.1038/srep37943. a.

Liu S, Su LC, Liu S, Zeng XJ, Zheng DM, ...Li L. Agrobacterium rhizogenes-mediated transformation of *Arachis hypogaea*: an efficient tool for functional study of genes. *BBEQ*. 2016; Online. doi:10.1080/13102818.2016.1191972. b.

Liu X, Chen CY, Wang KC, Luo M, Tai R, Yuan L, Zhao M, Yang S, Tian G, Cui Y, Hsieh HL, Wu K. PHYTOCHROME INTERACTING FACTOR3 associates with the histone deacetylase HDA15 in repression of chlorophyll biosynthesis and photosynthesis in etiolated Arabidopsis seedlings. Plant Cell. 2013; 25(4): 1258-73. doi: 10.1105/tpc.113.109710.

Luo M, Tai R, Yu CW, Yang S, Chen CY, Lin WD, Schmidt W, Wu K. Regulation of flowering time by the histone deacetylase HDA5 in Arabidopsis. Plant J. 2015; 82(6): 925-36. doi: 10.1111/tpj.12868.

Luo M, Wang YY, Liu X, Yang S, Lu Q, Cui Y, Wu K. (2012). HD2C interacts with HDA6 and is involved in ABA and salt stress response in Arabidopsis. J Exp Bot. 2012; 63(8): 3297-306. doi: 10.1093/jxb/ers059.

Ma X, Lv S, Zhang C, Yang C. Histone deacetylases and their functions in plants. Plant Cell

Rep. 2013; 32(4): 465-78. doi: 10.1007/s00299-013-1393-6.

Mikkelsen TS, Ku M, Jaffe DB, Issac B, Lieberman E, Giannoukos G, . . . Bernstein BE. Genome-wide maps of chromatin state in pluripotent and lineage-committed cells. Nature. 2007; 448(7153): 553-60. doi: 10.1038/nature06008.

Murfett J, Wang XJ, Hagen G, Guilfoyle TJ. Identification of Arabidopsis histone deacetylase HDA6 mutants that affect transgene expression. The Plant cell. 2001; 13(5): 1047-1061. doi: 10.1105/tpc.13.5.1047.

Muller PY, Janovjak H,Miserez AR, Dobbie Z. Processing of gene expression data generated by quantitative real-time RT-PCR. Biotechniques. 2002; 32: 1372–9. doi: 10.1093/bioinformatics/btg157.

Pandey R, Muller A, Napoli CA, Selinger DA, Pikaard CS, Richards EJ, Bender J, Mount DW, Jorgensen RA. Analysis of histone acetyltransferase and histone deacetylase families of Arabidopsis thaliana suggests functional diversification of chromatin modification amongmulticellular eukaryotes. Nucleic Acids Res. 2002; 30: 5036–55. doi: 10.1093/nar/gkf660.

Perrella G, Lopez-Vernaza MA, Carr C, Sani E, Gossele V, Verduyn C, Kellermeier F, Hannah MA, Amtmann A. Histone deacetylase complex1 expression level titrates plant growth and abscisic acid sensitivity in Arabidopsis. Plant Cell. 2013; 25(9): 3491-505. doi: 10.1105/tpc.113.114835.

Su LC, Deng B, Liu S, Li LM, Hu B, Zhong YT, Li L. Isolation and characterization of an osmotic stress and ABA induced histone deacetylase in Arachis hygogaea. Front Plant Sci. 2015; 6: 512. doi: 10.3389/fpls.2015.00512.

Tang Y, Liu X, Liu X, Li Y, Wu K, Hou X. Arabidopsis NF-YCs Mediate the Light-Controlled Hypocotyl Elongation via Modulating Histone Acetylation. Mol Plant. 2017; 10(2): 260-73. doi: 10.1016/j.molp.2016.11.007.

Tanaka M, Kikuchi A, Kamada H. The Arabidopsis histone deacetylases HDA6 and HDA19 contribute to the repression of embryonic properties after germination. Plant physiology. 2008; 146(1):149-161. doi: 10.1104/pp.107.111674.

Teranishi K. Development of imidazopyrazinone red-chemiluminescent probes for detecting superoxide anions via a chemiluminescence resonance energy transfer method. Luminescence. 2007; 22(2): 147-56. doi: 10.1002/bio.939.

Xing S, Poirier Y. The protein acetylome and the regulation of metabolism. Trends Plant Sci. 2012; 17(7): 423-30. doi: 10.1016/j.tplants.2012.03.008.

Yamamoto A, Hirouchi T, Kawamorita S, Nakashima K, Sugiyama A, Kato Y. Radioprotective activity of blackcurrant extract evaluated by *in vitro* micronucleus and gene mutation assays in TK6 human lymphoblastoid cells. Genes Environ. 2017; 39: 22. doi: 10.1186/s41021-017-0082-z.

Yang H, Liu X, Xin M, Du J, Hu Z, Peng H, Rossi V, Sun Q, Ni Z, Yao Y. Genome-Wide Mapping of Targets of Maize Histone Deacetylase HDA101 Reveals Its Function and Regulatory Mechanism during Seed Development. Plant Cell. 2016; 28(3): 629-45. doi: 10.1105/tpc.15.00691.

Yang P, Zhang F, Luo X, Zhou Y, Xie J. Histone deacetylation modification participates in the repression of peanut (Arachis hypogaea L.) seed storage protein gene *Ara h 2.02* during germination. Plant Biol (Stuttg). 2015; 17(2): 522-27. doi: 10.1111/plb.12268.

Yu CW, Chang KY, Wu, K. Genome-Wide Analysis of Gene Regulatory Networks of the FVE-HDA6-FLD Complex in Arabidopsis. Front Plant Sci. 2016; 7: 555. doi: 10.3389/fpls.2016.00555.

Yu CW, Liu X, Luo M, Chen C, Lin X, Tian G, Lu Q, Cui Y, Wu, K. HISTONE DEACETYLASE6 interacts with FLOWERING LOCUS D and regulates flowering in Arabidopsis. Plant Physiol. 2011; 156(1): 173-84. doi: 10.1104/pp.111.174417.

Zheng Y, Ding Y, Sun X, Xie S, Wang D, Liu X, Su L, Wei W, Pan L, Zhou DX. Histone deacetylase HDA9 negatively regulates salt and drought stress responsiveness in Arabidopsis. J Exp Bot. 2016; 67(6): 1703-13. doi: 10.1093/jxb/erv562.

Zheng YS, Lu YQ, Meng YY, Zhang RZ, Zhang H, Sun JM, Wang MM, Li HH, Li, RY. Identification of interacting proteins of the TaFVE protein involved in spike development in bread wheat. Proteomics. 2017; 17(9). doi: 10.1002/pmic.201600331.

Zhong R, Morrison WH 3rd, Himmelsbach DS, Poole FL 2nd, Ye ZH. Essential role of caffeoyl coenzyme A O-methyltransferase in lignin biosynthesis in woody poplar plants. Plant Physiol. 2000; 124(2): 563-78. doi: 10.1104/pp.124.2.563.

Preprints (www.preprints.org) | NOT PEER-REVIEWED | Posted: 25 September 2018 doi:10.20944/preprints201809.0486.v1

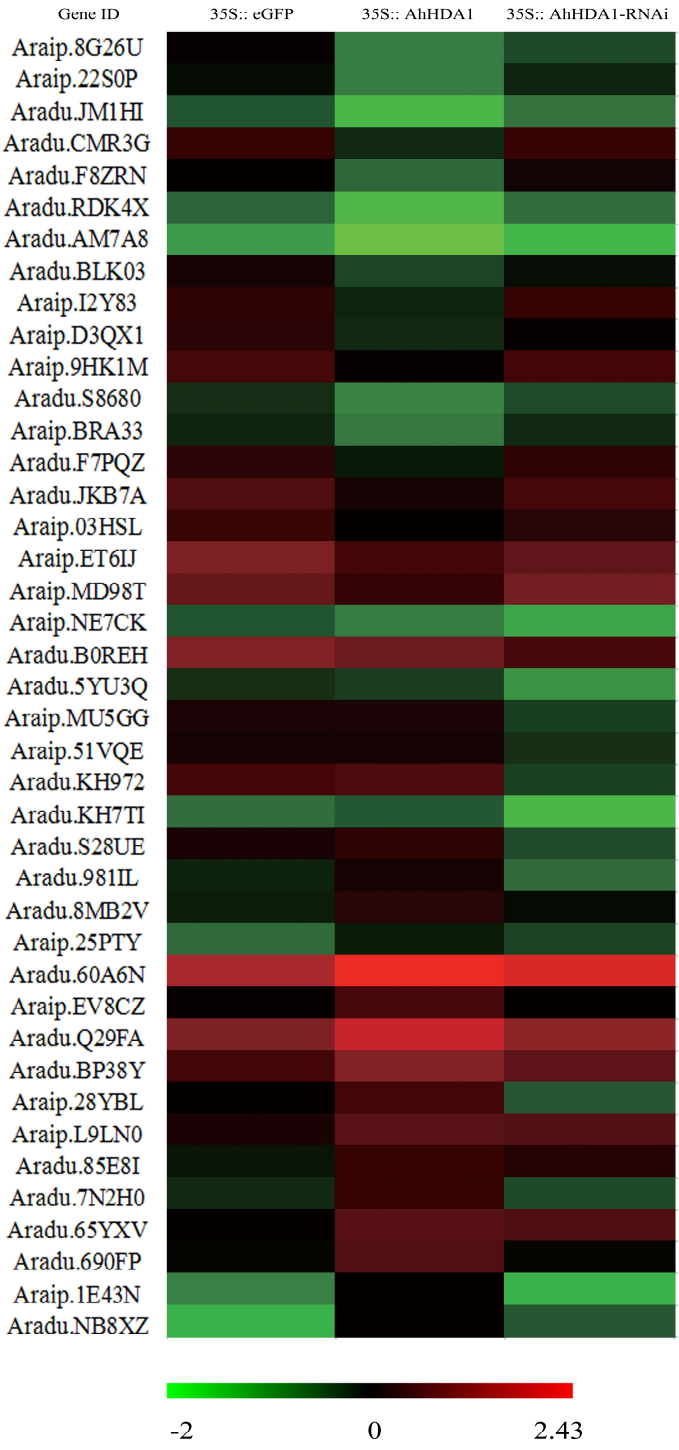

Fig S1. Heatmap of starch and sucrose metabolism pathway among different hairy roots.

Preprints (www.preprints.org) | NOT PEER-REVIEWED | Posted: 25 September 2018 doi:10.20944/preprints201809.0486.v1

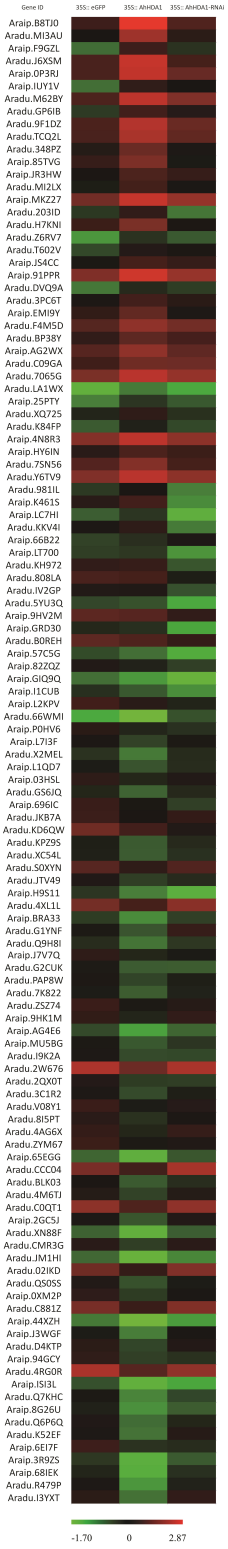

Fig S2. Heatmap of biomolecular synthesis pathway among different hairy roots.

Preprints (www.preprints.org) | NOT PEER-REVIEWED | Posted: 25 September 2018 doi:10.20944/preprints201809.0486.v1

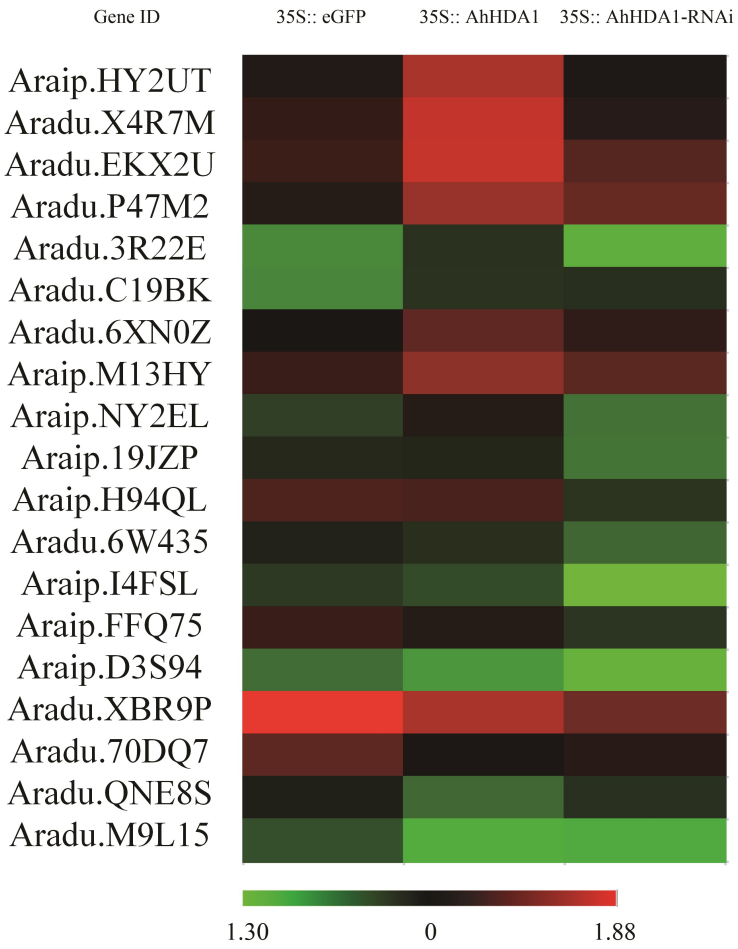

Fig S3. Heatmap of signal transduction pathway among different hairy roots.

Preprints (www.preprints.org) | NOT PEER-REVIEWED | Posted: 25 September 2018 doi:10.20944/preprints201809.0486.v1

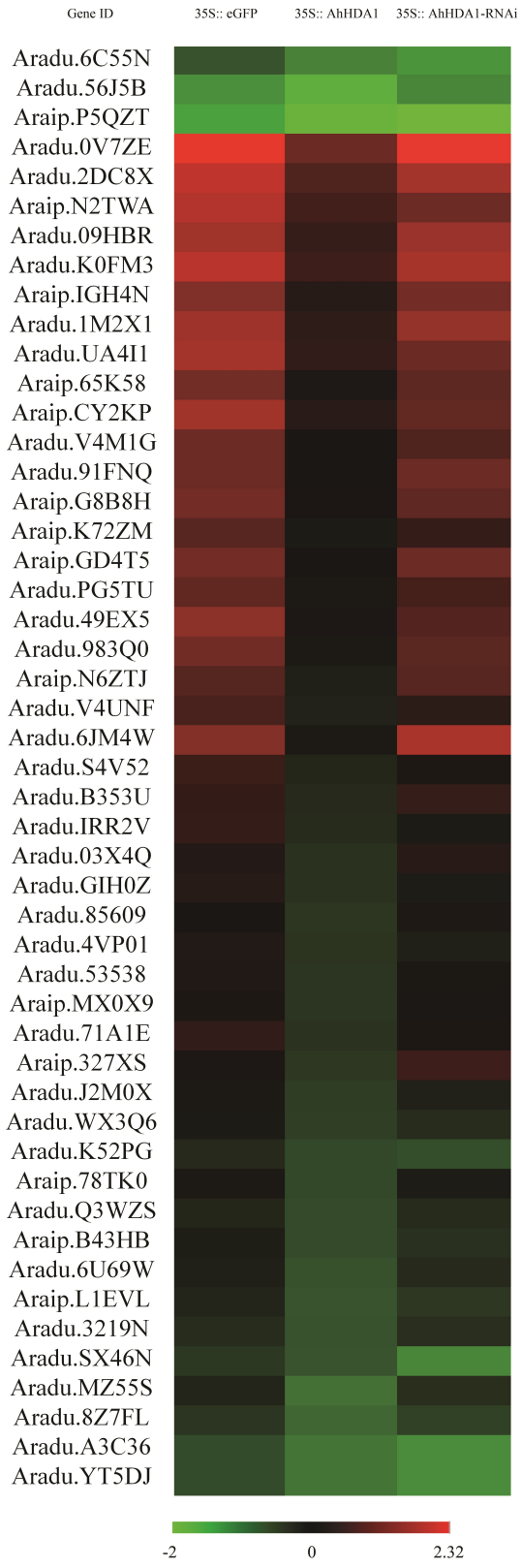

Fig S4. Heatmap of Photosynthesis and oxidative phosphorylation pathway among different hairy roots.

Preprints (www.preprints.org) | NOT PEER-REVIEWED | Posted: 25 September 2018 doi:10.20944/preprints201809.0486.v1

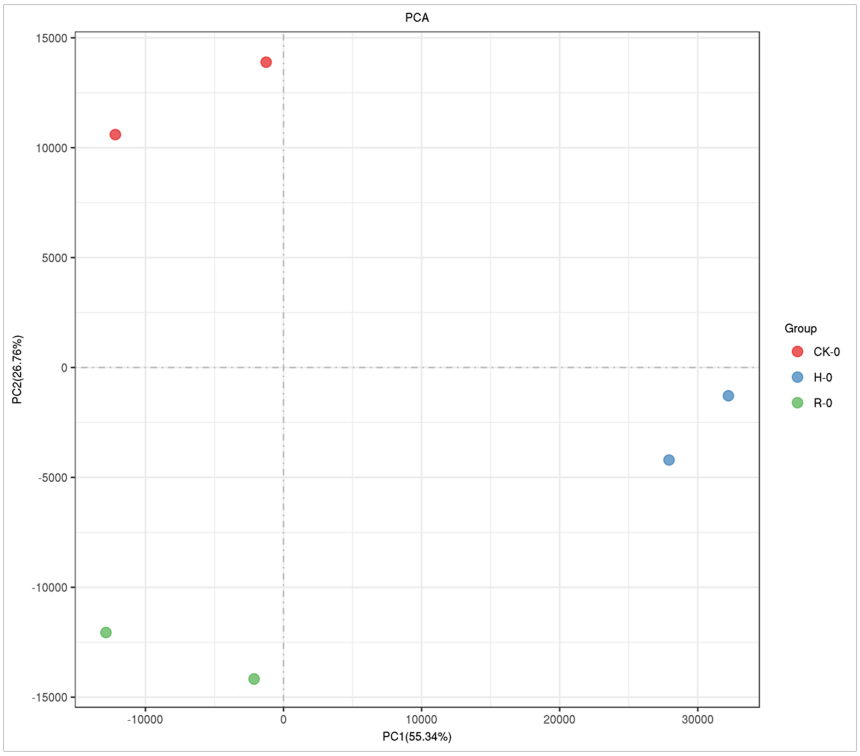

Fig S5. Principal components analysis of the gene transcript analysis in transgenic hairy roots.